Acta Crystallographica Section B
Structural Science
ISSN 0108-7681

π-Bond cooperativity and anticooperativity effects in resonance-assisted hydrogen bonds (RAHBs)

Valerio Bertolasi, Loretta Pretto, Gastone Gilli and Paola Gilli*

Centro di Strutturistica Diffrattometrica and Dipartimento di Chimica, Università di Ferrara, I-44100 Ferrara, Italy

Correspondence e-mail: paola.gilli@unife.it

Received 8 February 2006
Accepted 1 June 2006

Bond cooperativity effects, which are typical of 'resonant' chains or rings of π-conjugated hydrocarbons, can also occur in hydrogen-bonded systems in the form of σ-bond and π-bond cooperativity or anticooperativity. σ-Bond cooperativity is associated with the long chains of $O-H\cdots O$ bonds in water and alcohols while σ-bond anticooperativity occurs when the cooperative chain is interrupted by a local defect reversing the bond polarity. π-Bond cooperativity is the driving force controlling resonance-assisted hydrogen bonds (RAHBs), while π-bond anticooperativity has never been considered so far and is investigated here by studying couples of hydrogen-bonded β-enolone and/or β-enaminone six-membered rings fused through a common $C{=}O$ or $C-C$ bond. The effect is studied by X-ray crystal structure determination of five compounds [(2*Z*)-1-(2-hydroxyphenyl)-3-phenyl-1,3-propanedione enol (1), (2*Z*)-1-(2-hydroxy-5-chlorophenyl)-3-phenyl-1,3-propanedione enol (2), (2*Z*)-1-(2-hydroxy-5-methylphenyl)-3-phenyl-1,3-propanedione enol (3), (2*Z*)-1-(2-hydroxy-4-methyl-5-chlorophenyl)-3-phenyl-1,3-propanedione enol (4) and dimethyl(2*E*)-3-hydroxy-2-{[(4-chlorophenyl)amino]carbonyl}pent-2-enedioate (5)] and by extensive analysis of related fragments found in the CSD (Cambridge Structural Database). It is shown that fusion through the $C{=}O$ bond is always anticooperative and such to weaken the symmetric $O-H\cdots O\cdots H-O$ and $N-H\cdots O\cdots H-N$ bonds formed, but not the asymmetric $O-H\cdots O\cdots H-N$ bond. Fusion through the $C-C$ bond may produce either cooperative or anticooperative hydrogen bonds, the former being more stable than the latter and giving rise to a unique resonance-assisted ten-membered ring running all around the two fused six-membered rings, which can be considered a type of tautomerism never described before.

1. Introduction

The synergistic phenomenon by which a particular combination of chemical bonds may have a stabilization energy greater than the sum of the energies of the individual bonds is generally known as non-additivity or cooperativity. This effect is universally known as 'resonance' when associated with chains or rings of π-conjugated single and double bonds, but can occur in connection with other types of bond as well, and can be supposed to be 'particularly important in hydrogen bonding because of the diffuse nature and of the high polarizability of the hydrogen and lone-pair electron densities', as remarked by Jeffrey (1997), who also named 'σ-bond cooperativity' and 'π-bond cooperativity' the two different forms

doi:10.1107/S0108768106020933

by which this effect can strengthen the hydrogen bond itself (Jeffrey & Saenger, 1991).[1]

σ-Bond cooperativity (σ-cooperativity for short) involves the formation of homodromic chains (or cycles) of hydrogen bonds **1.Ia** that, for X = O and R = alkyl, aryl or H, describe the polymeric arrangements of alcohols, phenols and waters so frequently observed in crystals and that are known to determine a number of complex supramolecular assemblies in condensed phases [*e.g.* chlatrate hydrates (Jeffrey, 1984), cyclamers (Bertolasi & Ferretti, 2005), carbohydrates and their hydrates (Jeffrey & Saenger, 1991; Jeffrey, 1995, 1997)]. The effect was given this name (Jeffrey & Saenger, 1991) because it is attributable to the increased $X^{\delta-}{-}\mathrm{H}^{\delta+}$ polarization of the X—H σ-bond induced by cooperative hydrogen-bond formation, although other expressions, such as 'polarization (or induction)-assisted (or enhanced) hydrogen bond', have also been used (Jeffrey, 1995; Bertolasi *et al.*, 1996). Recent quantum-mechanical calculations (Scheiner, 1997; Kar & Scheiner, 2004) indicate that σ-cooperativity can provide hydrogen-bond energy enhancements up to 66% in long water chains with respect to water dimers. Homodromic σ-cooperative chains can be interrupted by local defects able to reverse the chain polarity (Saenger, 1979; Saenger *et al.*, 1982; Steiner, 2002), as shown in **1.Ib**, where the single point of σ-bond anticooperativity (σ-anticooperativity) is represented by the central water molecule marked in bold.

$\ldots X(R){-}H\ldots X(R){-}H\ldots X(R){-}H\ldots$ **1.Ia**

$\ldots H{-}(H)O\ldots H{-}(H)O\boldsymbol{\ldots H{-}O{-}H\ldots}O(H){-}H\ldots O(H){-}H\ldots$ **1.Ib**

$\ldots Y{=}R_n{-}X{-}H\ldots Y{=}R_n{-}X{-}H\ldots Y{=}R_n{-}X{-}H\ldots$ **1.II**

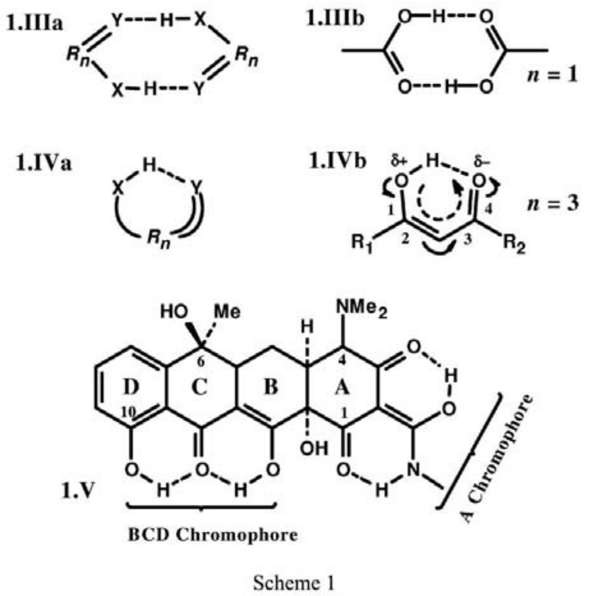

Scheme 1

The essential role played by σ-cooperative hydrogen bonds in nature is rather well known, infinite chains of hydrogen-bonded water molecules being the structure which guarantees the proton a mobility six times greater than that of any other cation in aqueous solutions by the so-called Grotthuss mechanism (de Grotthuss, 1806), while single-wire σ-cooperative proton-conducting chains of water molecules have been identified in the channels formed by gramicidin A, a helical pentadecapeptide behaving as a natural antibiotic against gram-positive bacteria by injecting protons through their cell membrane (Pomès & Roux, 2002; Duax *et al.*, 2003). More recently, it has been discovered that σ-anticooperative hydrogen bonds also play an essential role in aquaporins, a class of proteic channels crossing the cell membranes of all forms of life and having the function of providing water permeability while hindering proton transmission (Agre *et al.*, 1997). Here, two asparagine residues located midway along the channel have been shown (Tajkhorshid *et al.*, 2002) to stabilize a single point of σ-anticooperativity, so transforming the σ-cooperative water chain into two half-chains of opposite homodromicities (**1.Ib**), a structure that, although permitting fast water flow, can block proton transmission.

The second known type of hydrogen-bond cooperativity is π-bond cooperativity (π-cooperativity for short), which relies on the positive synergism between hydrogen-bond strengthening and π-delocalization enhancing that occurs when the hydrogen-bond donor and acceptor atoms are connected by a short chain of conjugated single and double bonds. This mechanism has been described as RAHB (resonance-assisted hydrogen bond; Gilli *et al.*, 1989, 1993, 1994, 2004; Bertolasi *et al.*, 1991) and can swell the hydrogen-bond energy with respect to the non-resonance-assisted structure much more efficiently than σ-cooperativity does, *e.g.* by three to four times in the case of O—H$\cdots$O bonds (Gilli, Ferretti & Gilli, 1996) and up to 2.5 times for the N—H$\cdots$O bonds (Kobko *et al.*, 2001; Kobko & Dannenberg, 2003). All π-cooperative RAHBs can be reduced to the formula $\cdots Y{=}R_n{-}X\mathrm{H}\cdots$ where X and Y are the hydrogen-bond donor and acceptor atoms and R_n (n odd) is a resonant spacer of n atoms forming a short chain of alternating single and double bonds, *e.g.* n = 1 in carboxylic acids ($\cdots$O=C—OH$\cdots$) and amides ($\cdots$O=C—NH$\cdots$), n = 3 in β-diketone enols ($\cdots$O=C—C=C—OH$\cdots$), β-enaminones ($\cdots$O=C—C=C—NH$\cdots$) and keto-hydrazones ($\cdots$O=C—C=N—NH$\cdots$), and, respectively, n = 5 and 7 in the few cases of hydrogen-bonded δ- and ζ-diketone enols known so far (Gilli & Bertolasi, 1990; Bertolasi *et al.*, 1995; Gilli, Ferretti, Bertolasi & Gilli, 1996; Gilli, Ferretti & Gilli, 1996; Gilli & Gilli, 2000; Gilli *et al.*, 2002). Intermolecular RAHBs give rise to chains (**1.II**) or dimers (**1.IIIa,b**) of hydrogen-bonded molecules, while intramolecular RAHBs produce hydrogen-bonded rings **1.IVa**, which frequently assume, for n = 3, the form of the six-membered hydrogen-bonded ring typical of β-diketone enols (or enolones), **1.IVb**. π-Cooperative hydrogen bonds are of particular importance in chemistry, where they are at the very root of the phenomenon of keto–enol tautomerism, and may have remarkable implications in biochemistry because α-helices or β-pleated sheets,

---

[1] Very recently, a hybrid π- and σ-cooperativity has also been proposed by the Nangia group (Vishweshwar *et al.*, 2004) and named synthon-assisted hydrogen bond (SAHB).

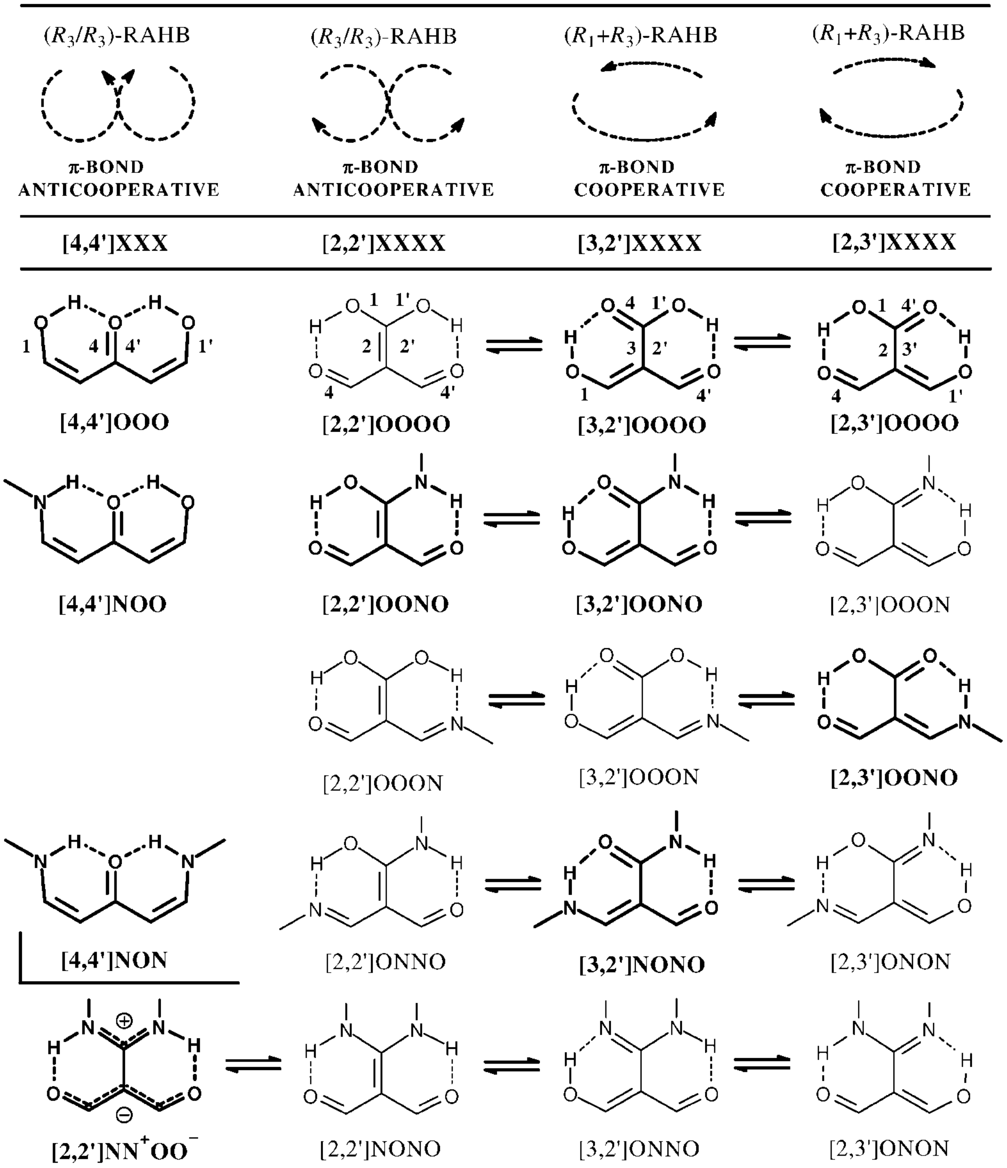

Figure 1
'Theoretical' relationships of π-bond coooperativity and anticooperativity in the fusion of two enolone and/or enaminone fragments forming intramolecular R_3-RAHB rings. Numbering as 1–4 the covalent bonds, four different junctions ([4,4′], [2,2′], [3,2′] and [2,3′]) are possible, each having the hydrogen bonds in different positions. Schemes drawn in bold correspond to patterns actually found in practice.

the determinants of the secondary structure of proteins, are actually chains of RAHB-connected amide groups, while thymine–adenine and cytosine–guanine couples in DNA are also linked by resonance-assisted hydrogen bonds (Gilli *et al.*, 1989; Gilli, Ferretti, Bertolasi & Gilli, 1996).

RAHB is a natural π-cooperative system and, to our knowledge, its π-anticooperative effects have never been discussed as such, although RAHB patterns arranged in an anticooperative way are sometimes observed in both synthetic and natural products, where they are normally associated with complex tautomeric motifs. Good examples are tetracycline antibiotics (**1.V**) which include two different moieties, known as BCD and A chromophores, of adjacent RAHB rings whose hydrogen bonds can be weakened (or strengthened) by mutual π-anticooperativity (or π-cooperativity) relationships. Both chromophores are reportedly implicated in the binding to the 30S ribosomal subunit of tetracycline drugs able to inhibit the bacterial proteic synthesis (Brodersen *et al.*, 2000), while chromophore A has been proposed to play an important role in the complex scheme of protonation and isomerization reactions occurring in these compounds (Gilli & Bertolasi, 1990).

This paper tries to address, in a systematic way, π-cooperative and anticooperative effects arising from the fusion of two intramolecular R_3-RAHB rings forming O—H···O, N—H···O and O—H···N bonds. Even by restricting all atoms of the resonant spacer to C atoms, the number of combination patterns (Fig. 1) remains relevant because:

(i) the heteroatoms can be associated in two different ways (*XXX* and *XXXX*, *X* = O, N);

(ii) the chemical bonds of the two hydrogen-bonded rings can have four distinct types of junction ([4,4′], [2,2′], [3,2′] and [2,3′]);

(iii) the two fused R_3-RAHB rings may be in mutual relationships of π-anticooperativity (R_3/R_3) or π-cooperativity (R_1 + R_3), as indicated at the top of Fig. 1 by the direction of the dashed arrows marking the sense of RAHB π-electron delocalization.

The present paper is aimed at verifying whether the 'theoretical' combination patterns of Fig. 1 do actually exist in nature. This will be accomplished through an extensive analysis of crystal structures, either newly determined or retrieved from the Cambridge Structural Database (CSD) (Allen, 2002), of chemical compounds which contain the patterns investigated as molecular subfragments. It will be shown that only some of the possible tautomeric forms (marked in bold in the figure) do actually occur in practice, mainly because of the different N—H···O and O—H···N stabilities, and that the relative occurrences of the different forms can be convincingly rationalized in terms of two concepts: (i) RAHB synergism of hydrogen-bond strengthening and π-delocalization; and (ii) equalization of the PA/pK_a values of the hydrogen-bond donor and acceptor groups.

2. Data retrieval

At variance with Fig. 1, which shows the π-cooperative and anticooperative patterns predictable 'in theory', Schemes 2*A* and 2*B* report only those actually found in real crystal structures. The patterns are arranged in classes (from **2.I** to **2.VII**) whose most significant average geometrical parameters are given in Table 1, while some representative compounds are illustrated, in stick and ball style, in Scheme 3.[2]

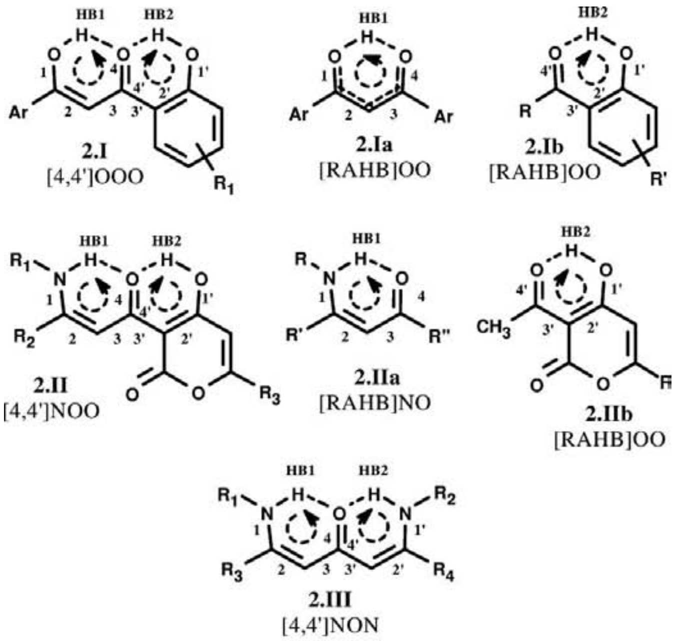

Scheme 2*A*

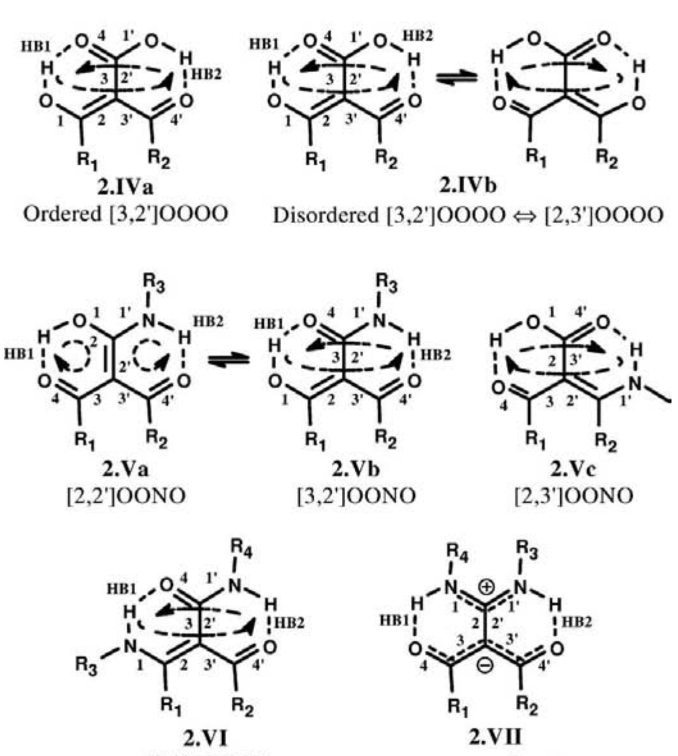

Scheme 2*B*

All structures were retrieved from the CSD with the exception of (1)–(5) (Scheme 4), determined by X-ray diffraction in our laboratory. Four of them are compounds of type **2.I**, *i.e.* (2*Z*)-1-(2-hydroxyphenyl)-3-phenyl-1,3-propanedione enol (1); (2*Z*)-1-(2-hydroxy-5-chlorophenyl)-3-phenyl-1,3-propanedione enol (2); (2*Z*)-1-(2-hydroxy-5-methylphenyl)-3-phenyl-1,3-propanedione enol (3); and (2*Z*)-1-(2-hydroxy-4-methyl-5-chlorophenyl)-3-phenyl-1,3-propanedione enol (4). The crystal structure of (5) (dimethyl-(2*E*)-3-hydroxy-2-{[(4-chlorophenyl)amino]carbonyl}pent-2-enedioate) was determined at 100 K to obtain a better localization of the hydrogen-bonded proton in a class of molecules

---

[2] Chemical formulae, chemical names and references for compounds of Scheme 3: **3.I** YAVROC, $C_{16}H_{14}O_4$, (*Z*)-3-(2-hydroxyphenyl)-1-(4-methoxyphenyl)-3-oxo-prop-1-en-1-ol (Cox *et al.*, 1993); **3.II** LOMYER, $C_{18}H_{17}N_1O_6$, ethyl 2-anilino-4-(4-hydroxy-6-methyl-2-oxo-2*H*-pyran-3-yl)-4-oxo-2-butenoate (Brbot-Šaranović *et al.*, 2000); **3.III** KUSBAB, $C_{18}H_{18}N_2O_1$, 1-amino-5-(*N*-phenylamino)-1-phenylhexa-1,4-dien-3-one (Bartoli *et al.*, 1992); **3.IVa** CITNIN02, $C_{13}H_{14}O_5$, citrinin (Destro & Marsh, 1984); **3.IVa′** FACVUB, $C_{12}H_{11}N_1O_4$, 1-ethyl-4-hydroxy-2-oxo-1,2-dihydroquinoline-3-carboxylic acid (Shishkina *et al.*, 2002); **3.IVb** KUXMAR, $C_{14}H_8O_4$, 2-carboxy-3-hydroxyphenalen-1-one (Sugawara *et al.*, 1992); **3.IVb′** SUGCEC, $C_{16}H_{10}O_4$, 7-hydroxy-5-oxo-5*H*-dibenzo[*a*,*c*][7]annulene-6-carboxylic acid (Mochida *et al.*, 1992); **3.Va** XAYCAB, $C_{22}H_{25}N_2O_8^+Cl^-$, tetracycline hydrochloride (Clegg & Teat, 2000); **3.Va′** QECQAQ, $C_{13}H_{13}N_1O_5$, 2,2-dimethyl-5-(*N*-phenylamino-(hydroxy)methylene)-1,3-dioxane-4,6-dione (Mukhopadhyaya *et al.*, 2000*a*); **3.Vb** BINNAN, $C_{20}H_{20}N_2O_8$, 5a-epi-6-oxatetracycline (Kollat & Stezowski, 1982); **3.Vb′** NOZLAP, $C_{26}H_{19}N_1O_3$, 2-benzoyl-3-hydroxy-1(1-naphtylamino)-3-phenyl-2-propen-1-one (Ozturk *et al.*, 1998); **3.Vb″** KOBZOQ, $C_{22}H_{20}N_4O_4$, 4-hydroxy-1-methyl-2-oxo-*N*-(4-oxo-2-propyl-3,4-dihydroquinazolin-3-yl)-1,2-dihydroquinoline-3-carboxamide (Shishkina *et al.*, 2000); **3.VI** DIHRUH10, $C_6H_{10}N_2O_2$, 3-amino-2-formyl-*N*-methylbut-2-enamide (Takahashi *et al.*, 1989); **3.VII** AMIMZA10, $C_8H_{12}N_2O_2$, 3-(2-imidazolidinylidene)-2,4-pentanedione (Adhikesavalu & Venkatesan, 1983).

(**2.Va** or **b**, see below) where its position within the very short O—H···O bond was unclear. Details on crystal structure determination and refinement are given in §4.

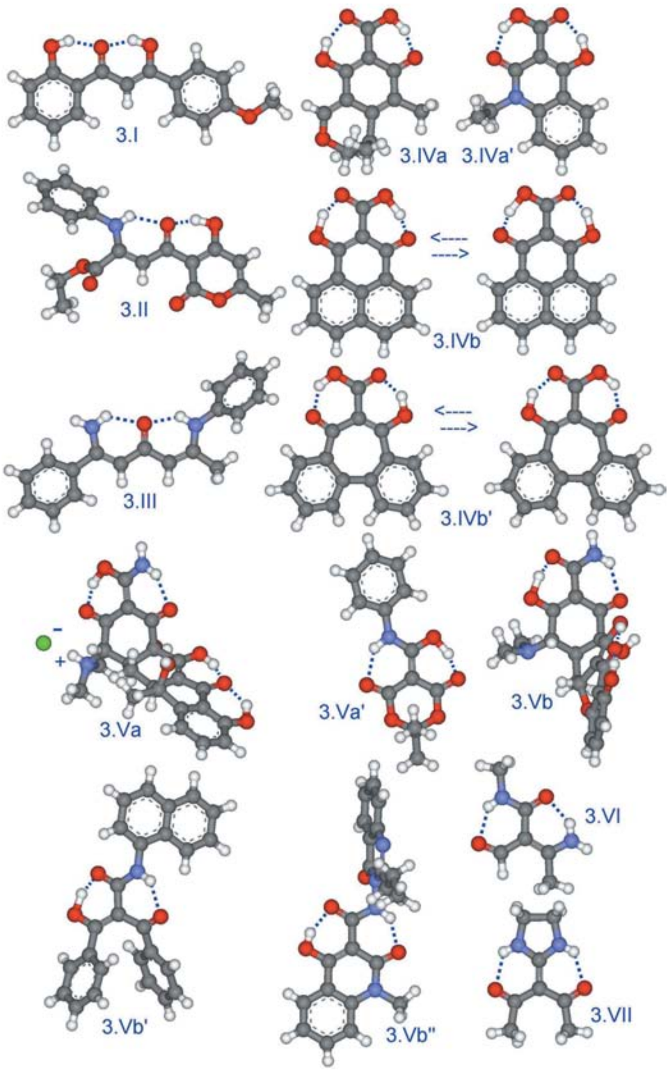

Scheme 3

Patterns [n,n′]XXX, Scheme 2(A). Intramolecular π-anticooperativity has been studied in more detail for the [4,4′]OOO pattern, by taking advantage of the fact that 1-(2-hydroxyphenyl)-3-phenyl-1,3-propanedione enols (**2.I** and **3.I**) can be considered to derive from [4,4′] fusion of dibenzoylmethane enols **2.Ia** [a class of molecules well known to give some of the strongest O—H···O RAHBs (Gilli *et al.*, 1994)] with 1-(2-hydroxyphenyl)-alkyl-1-ones **2.Ib**. The working hypothesis was that the two O—H···O RAHBs in **2.Ia** and **2.Ib** could be mutually weakened when forming **2.I** because the two hydrogen bonds are in position to compete for the same central carbonyl bond. Compounds of type **2.I** include the four structures (1)–(4) and two more CSD structures (Cox *et al.*, 1993; Ng *et al.*, 1994), while seven high-quality structures of strong single-well RAHBs (Gilli *et al.*, 2004) and a wide set of 66 CSD structures (Table S1 of the supplementary material)[3] were used to define the geometries of subfragments **2.Ia** and **2.Ib**, respectively.

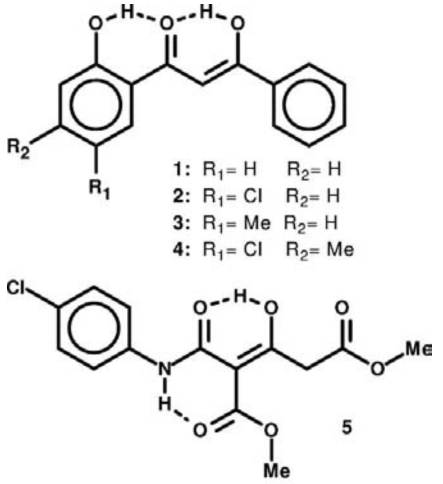

Scheme 4

The six compounds containing the anticooperative [4,4′]NOO pattern (**2.II** and **3.II**) belong to a rather uniform series of structures determined in the same laboratory (Brbot-Šaranović *et al.*, 2000, 2001; Cindrić *et al.*, 2002). They can be thought of as arising from the [4,4′] fusion of the simple enaminones **2.IIa** with 3-acetyl-4-hydroxy-pyran-2-ones **2.IIb**. Their average geometries were established from the only three structures available for **2.IIb** (Thailambal & Pattabhi, 1985; Shuxiang *et al.*, 1990; Bertolasi *et al.*, 1997) and from a much larger set of 50 structures for **2.IIa** (Table S2 of the supplementary material).[3]

Finally, four compounds were found to correspond to the anticooperative [4,4′]NON scheme (**2.III** and **3.III**; Himmelsbach *et al.*, 1987; Bartoli *et al.*, 1992).

Patterns [n,n′]XXXX, Scheme 2(B). Out of the 15 possible patterns of Fig. 1, the seven which contain one or two O—H···N bonds have never been observed because of the greater stability of the N—H···O tautomers (see below). As far as the potential [2,2′]OOOO ⇌ [3,2′]OOOO ⇌ [2,3′]OOOO tautomery of Table 1 is concerned, the anticooperative [2,2′]OOOO pattern is never found, the other two tautomers always being preferred (**2.IVa**,**b**). Hydrogen-bonded protons are ordered (**2.IVa**) in citrinin at 19 and 147 K (**3.IVa**; Destro & Marsh, 1984; Destro, 1991; Roversi *et al.*, 1996) and in a single room-temperature structure (**3.IVa′**; Shishkina *et al.*, 2002), while dynamic disorder (**2.IVb**) is observed in citrinin at 295 K (Destro & Marsh, 1984) and in three other structures determined between 130 and 295 K (**3.IVb** and **3.IVb′**; Sugawara *et al.*, 1992; Mochida *et al.*, 1992; Duncan *et al.*, 2002).

Compounds associated with the tautomeric equilibrium [2,2′]OONO ⇌ [3,2′]OONO (**2.Va**,**b**) correspond in five cases to the first tautomer (**2.Va**; **3.Va**,**a′**) (Bordner, 1979; Koziol *et*

---

[3] Supplementary data for this paper are available from the IUCr electronic archives (Reference: DE5027). Services for accessing these data are described at the back of the journal.

Table 1
Average O···O and N···O contact distances (Å), C—C, C—O and C—N bond lengths (Å) and Pauling's bond numbers n (in italic) for the RAHB patterns of Schemes 2(A) and 2(B).

The indices ⟨λ⟩ ($0 \le \lambda \le 1$) and Del% = 100 (1 − |2⟨λ⟩ − 1|) ($0 \le$ Del% ≤ 100) are a measure of the delocalization of the π-conjugated fragment due to resonance between the two HX—C=C—C=Y ↔ X=C—C=C—YH VB canonical forms typical of RAHB (λ = 0.5 and Del% = 100 for complete π-delocalization). N is the number of crystal structures in the sample.

Class	Pattern	HB1	HB2	d_1	d_2	d_3	d_4	$d_{1'}$	$d_{2'}$	$d_{3'}$	$d_{4'}$	N	Reference†
Scheme 2A													
2.I	[4,4′]OOO	**2.53 (1)**	**2.58 (1)**	1.32 (1)	1.36 (1)	1.43 (1)	1.27 (1)	1.35 (1)	1.41 (1)	1.47 (1)	$\equiv d_4$	9	pw, a1–a2
	Anticooperative			*1.24*	*1.77*	*1.30*	*1.54*	*1.12*	*1.42*‡	*1.08*			
				$\langle\lambda\rangle_{1\text{-}4}$ = 0.28, Del% = 56				**$\langle\lambda\rangle_{1'\text{-}4'}$ = 0.11, Del% = 22**					
2.Ia	[RAHB]OO	**2.46 (1)**		1.31 (2)	1.38 (1)	1.41 (1)	1.28 (1)					7	b
				1.31	*1.61*	*1.41*	*1.47*						
				$\langle\lambda\rangle_{1\text{-}4}$ = 0.41, Del% = 82									
2.Ib	[RAHB]OO		**2.51 (3)**					1.35 (1)	1.41 (2)	1.47 (2)	1.24 (1)	66	c
								1.12	*1.41*‡	*1.09*	*1.71*		
								$\langle\lambda\rangle_{1'\text{-}4'}$ = 0.16, Del% = 30					
2.II	[4,4′]NOO	**2.65 (4)**	**2.42 (2)**	1.33 (1)	1.39 (1)	1.41 (2)	1.30 (2)	1.31 (1)	1.39 (1)	1.46 (1)	$\equiv d_4$	6	d1–d3
	Anticooperative			*1.49*	*1.54*	*1.41*	*1.36*	*1.31*	*1.54*	*1.12*			
				$\langle\lambda\rangle_{1\text{-}4}$ = 0.44, Del% = 88				**$\langle\lambda\rangle_{1'\text{-}4'}$ = 0.29, Del% = 58**					
2.IIa	[RAHB]NO	**2.66 (3)**		1.34 (2)	1.38 (2)	1.42 (2)	1.25 (1)					50	e
				1.41	*1.61*	*1.35*	*1.65*						
				$\langle\lambda\rangle_{1\text{-}4}$ = 0.38, Del% = 76									
2.IIb	[RAHB]OO		**2.47 (1)**					1.31 (1)	1.40 (1)	1.44 (1)	1.24 (1)	5	f1–f3
								1.33	*1.47*	*1.23*	*1.69*		
								$\langle\lambda\rangle_{1'\text{-}4'}$ = 0.35, Del% = 70					
2.III	[4,4′]NON	**2.67 (2)**	**2.65 (2)**	1.35 (1)	1.35 (1)	1.44 (1)	1.28 (1)	1.35 (1)	1.36 (1)	1.43 (1)	$\equiv d_4$	4	g1–g2
	Anticooperative			*1.36*	*1.83*	*1.24*	*1.47*	*1.36*	*1.77*	*1.30*			
				$\langle\lambda\rangle_{1\text{-}4}$ = 0.26, Del% = 52				**$\langle\lambda\rangle_{1'\text{-}4'}$ = 0.29, Del% = 58**					
Scheme 2B													
2.IVa	[3,2′]OOOO	**2.54 (1)**	**2.48 (2)**	1.33 (1)	1.38 (1)	1.47 (1)	1.24 (1)	1.31 (1)	$\equiv d_3$	1.44 (1)	1.27 (1)	3	h1–h4
	Cooperative			*1.23*	*1.58*	*1.08*	*1.72*	*1.29*		*1.24*	*1.54*		
	Ordered			**$\langle\lambda\rangle_{1,2,3',4',1',4}$ = 0.32, Del% = 64**									
2.IVb	[3,2′]OOOO	**2.50 (5)**	**2.48 (5)**	1.28 (2)	1.40 (1)	1.47 (1)	1.26 (1)	1.28 (1)	$\equiv d_3$	1.41 (1)	1.28 (1)	5	h1, i1–i3
	Cooperative			*1.47*	*1.48*	*1.09*	*1.59*	*1.47*		*1.41*	*1.47*		
	Disordered			**$\langle\lambda\rangle_{1,2,3',4',1',4}$ = 0.47, Del% = 94**									
2.Va	[2,2′]OONO	**2.48 (2)**	**2.70 (3)**	1.30 (1)	1.42 (1)	1.42 (1)	1.25 (1)	1.33 (2)	$\equiv d_2$	1.46 (2)	1.23 (1)	5	l1–l5
	Anticooperative			*1.36*	*1.35*	*1.35*	*1.65*	*1.49*		*1.35*	*1.78*		
				$\langle\lambda\rangle_{1\text{-}4}$ = 0.35, Del% = 70				**$\langle\lambda\rangle_{1'\text{-}4'}$ = 0.35, Del% = 70**					
2.Vb	[3,2′]OONO	**2.44 (3)**	**2.66 (4)**	1.29 (2)	1.40 (2)	1.46 (1)	1.27 (2)	1.33 (2)	$\equiv d_3$	1.44 (1)	1.23 (4)	18	pw, m1–m14
	Cooperative			*1.41*	*1.48*	*1.14*	*1.53*	*1.49*		*1.24*	*1.78*		
				$\langle\lambda\rangle_{1,2,3',4',1',4}$ = 0.39, Del% = 78									
2.Vc	[2,3′]OONO	**2.54**	**2.66**	1.33	1.47	1.44	1.25	1.32	1.40	$\equiv d_2$	1.24	1	n
	Cooperative			*1.21*	*1.09*	*1.24*	*1.65*	*1.56*	*1.48*		*1.71*		
				$\langle\lambda\rangle_{1,4',1',2',3,4}$ = 0.36, Del% = 72									
2.VI	[3,2′]NONO	**2.59 (1)**	**2.66 (1)**	1.32 (1)	1.39 (2)	1.48 (1)	1.25 (1)	1.33 (1)	$\equiv d_3$	1.44 (2)	1.23 (1)	2	o1–o2
	Cooperative			*1.56*	*1.54*	*1.04*	*1.65*	*1.49*		*1.24*	*1.78*		
				$\langle\lambda\rangle_{1,2,3',4',1',4}$ = 0.39, Del% = 72									
2.VII	[2,2′]NN$^+$OO$^-$	**2.66 (5)**	**2.66 (5)**	1.33 (1)	1.43 (1)	1.43 (1)	1.23 (1)	1.34 (1)	$\equiv d_2$	1.44 (1)	1.23 (1)	4	p1–p2
	Proton transfer			*1.49*	*1.30*	*1.30*	*1.78*	*1.41*		*1.24*	*1.23*		
				$\langle\lambda\rangle_{1\text{-}1'}$ = 0.46, Del% = 92				**$\langle\lambda\rangle_{4\text{-}3\text{-}3'\text{-}4'}$ = 0.50, Del% = 100**					

† (a1) Cox *et al.* (1993); (a2) Ng *et al.* (1994); (b) Gilli *et al.* (2004); (c) Table S1 of the supplementary material; (d1) Brbot-Šaranović *et al.* (2000); (d2) Brbot-Šaranović *et al.* (2001); (d3) Cindrić *et al.* (2002); (e) Table S2 of the supplementary material; (f1) Thailambal & Pattabhi (1985); (f2) Shuxiang *et al.* (1990); (f3) Bertolasi *et al.* (1997); (g1) Himmelsbach *et al.* (1987); (g2) Bartoli *et al.* (1992); (h1) Destro & Marsh (1984); (h2) Destro (1991); (h3) Roversi *et al.* (1996); (h4) Shishkina *et al.* (2002); (i1) Sugawara *et al.* (1992); (i2) Mochida *et al.* (1992); (i3) Duncan *et al.* (2002); (l1) Bordner (1979); (l2) Koziol *et al.* (1992); (l3) de C. T. Carrondo *et al.* (1994); (l4) Clegg & Teat (2000); (l5) Mukhopadhyaya *et al.* (2000*a*); (m1) Von Dreele & Hughes (1971); (m2) Stezowski (1976); (m3) Palenik *et al.* (1978); (m4) Prewo *et al.* (1980); (m5) Prewo & Stezowski (1980); (m6) Kollat & Stezowski (1982); (m7) Silverton *et al.* (1982); (m8) Ried *et al.* (1985); (m9) Bossio *et al.* (1993); (*m*10) Ozturk *et al.* (1998); (*m*11) Shishkina *et al.* (2000); (*m*12) Ukrainets, Taran, Likhanova, Amin & Shishkin (2000); (*m*13) Ukrainets, Taran, Likhanova, Rybakov *et al.* (2000); (*m*14) Mukhopadhyaya *et al.* (2000*b*); (n) Wiley *et al.* (1986); (o1) Takahashi *et al.* (1989); (o2) Mehdi (1990); (p1) Adhikesavalu & Venkatesan (1983); (p2) Bernhardt *et al.* (2002). ‡ C—C bonds making part of aromatic rings with equilibrium bond number n = 1.50.

al., 1992; de C. T. Carrondo *et al.*, 1994; Clegg & Teat, 2000; Mukhopadhyaya *et al.*, 2000*a*) and in 18 cases to the second tautomer (**2.Vb**; **3.Vb**,**b′**,**b″**) (Von Dreele & Hughes, 1971; Stezowski, 1976; Palenik *et al.*, 1978; Prewo *et al.*, 1980; Prewo & Stezowski, 1980; Kollat & Stezowski, 1982; Silverton *et al.*, 1982; Ried *et al.*, 1985; Bossio *et al.*, 1993; Ozturk *et al.*, 1998; Shishkina *et al.*, 2000; Ukrainets, Taran, Likhanova, Amin & Shishkin, 2000; Ukrainets, Taran, Likhanova, Rybakov *et al.*, 2000; Mukhopadhyaya *et al.*, 2000*b*). The third non-tautomeric isomer [2,3′]OONO (**2.Vc**) was observed only once (Wiley *et al.*, 1986). All these compounds belong to a number of different chemical classes, the R_1 and R_2 substituents being non-annulated (**3.Vb′**), mono-annulated (**3.Vb**), bi-annulated (**3.Vb″**) and tetra-annulated (tetracyclines) (**3.Va**) in three, five, two and 13 cases, respectively.

Finally, only two structures containing the [3,2′]NONO pattern (**2.VI** and **3.VI**) were retrieved (Takahashi *et al.*, 1989; Mehdi, 1990), while the [2,2′]NONO pattern, which should be the stable isomer of the [2,2′]NONO $\rightleftharpoons$ [3,2′]ONNO $\rightleftharpoons$ [2,3′]ONON equilibrium because of its lack of O—H···N bonds, is never found because all three compounds identified (Adhikesavalu & Venkatesan, 1983; Bernhardt *et al.*, 2002) assume the zwitterionic form [2,2′]NN$^+$OO$^-$ (**2.VII** and **3.VII**).

The average geometrical parameters of compounds **2.I**–**2.VII** of Schemes 2*A* and 2*B* are given in Table 1. They include hydrogen-bond O···O and N···O contact distances and lengths of all C—C, C—O and C—N bonds of the resonant ···*Y*═C—C═C—*X*H··· fragment together with their average Pauling's bond numbers, n ($1 \leq n \leq 2$) (Pauling, 1947, 1960), and fragment π-delocalization indices.[4] These delocalization indices, $\langle\lambda\rangle$ ($0 \leq \langle\lambda\rangle \leq 1$) (Gilli *et al.*, 2004) and Del% = $100\,(1 - |2\langle\lambda\rangle - 1|)$, have the following meaning. With reference to the two extreme ···*Y*═C—C═C—*X*H··· (EK, enol–ketonic) and ···H*Y*—C═C—C═*X*··· (KE, keto–enolic) forms, the two unperturbed single- and double-bond geometries have the same Del% = 0 for $\langle\lambda\rangle$ of 0 and 1 for EK and KE, respectively, while the completely π-delocalized structure resulting from 1:1 VB (valence-bond) resonance mixing has Del% = 100 for a $\langle\lambda\rangle$ value of 0.5. Del% is, therefore, the simplest and most straightforward measure of the percent delocalization induced by RAHB in the resonant fragment.

3. Data analysis

3.1. Ring fusion through the C═O bond

[4,4′]OOO (2.I). These compounds form the simple [4,4′]OOO pattern, where anticooperativity effects on hydrogen-bond strength and π-delocalization can be highlighted by comparison with the structures of **2.Ia** and **2.Ib** (Scheme 2*A* and Table 1), from which they derive through [4,4′] fusion of their C═O bonds. Both O···O distances HB1 = 2.46 Å in **2.Ia** and HB2 = 2.51 Å in **2.Ib** are increased to 2.53 and 2.58 Å in **2.I**, with a lengthening of some 0.07 Å for both bonds. Also the average percent delocalizations, Del%, are decreased by the anticooperative fusion from 82 to 56 in **2.Ia** and from 30 to 22 in **2.Ib**, indicating a general loss of π-conjugation. These conclusions are supported by the $d_{\mathrm{O}\cdots\mathrm{O}}$(HB2) *versus* $d_{\mathrm{O}\cdots\mathrm{O}}$(HB1) scatterplot of Fig. 2, where full points and open diamonds indicate present and literature data, and the open square represents the average of values for the non-fused rings **2.Ia** and **2.Ib**. The two hydrogen-bond distances are positively correlated, a feature to be considered specific of π-bond anticooperativity effects because it is at variance with that observed for all other types of three-centre hydrogen bonds, where the shortening of one bond is always associated with the lengthening of the other, and *vice versa* (Taylor *et al.*, 1983; Taylor & Kennard, 1984; Steiner & Saenger, 1992; Jeffrey, 1995).

The anticooperativity effect can be attributed to the competition of the two resonant hydrogen bonds for the same central C═O bond (see **2.I**), whose π-delocalizability is necessarily limited. Moreover, since both fused RAHBs derive from the *R*—CO—CH*R*—CO—*R* $\rightleftharpoons$ *R*—CO—CR═C(OH)—*R* keto–enol tautomerism (a form of C-tautomerism) shifted to the right by RAHB stabilization, the anticooperative [4,4′]OOO energy destabilization could be such as to break one hydrogen bond (*e.g.* HB1 in **2.I**) and to bring back the corresponding enol to its Ar—CO—CH*R*—CO—Ar diketonic form. This possibility has been checked by a full CSD search, which has shown that there is only one example (Cunningham *et al.*, 1989) of such a chemical configuration not certainly ascribable to sheer steric repulsion. It may then be concluded that the accumulation of two weaker RAHBs is still more stable than just one stronger RAHB.

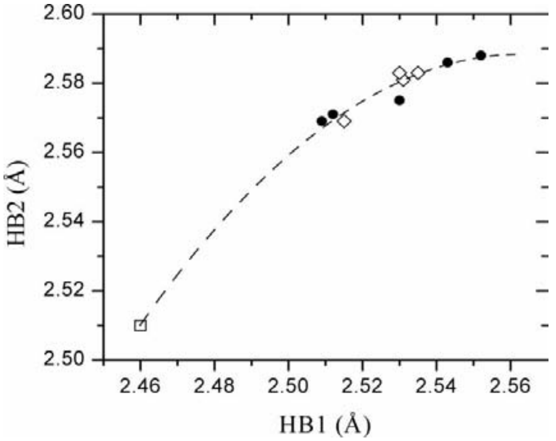

Figure 2
Plot of $d_{\mathrm{O}\cdots\mathrm{O}}$(HB2) *versus* $d_{\mathrm{O}\cdots\mathrm{O}}$(HB1) for compounds **2.I** forming the π-bond anticooperative pattern [4,4′]OOO. Full points and open diamonds indicate present and literature crystal structures, respectively, and the open square represents the averaged values derived from the non-fused rings **2.Ia** and **2.Ib**.

---

[4] Pauling's bond numbers n ($1 \leq n \leq 2$) were calculated as $d(1) - d(n) = c \log_{10} n$. Values for pure single ($n = 1$) and double ($n = 2$) bond distances used in the calculations are (1.49–1.33), (1.38–1.20) and (1.41–1.27) Å for Csp^2—Csp^2, Csp^2—O and Csp^2—Nsp^2 bonds, respectively. Reference C—C aromatic bonds were taken as having $d = 1.394$ Å for $n = 1.50$. The average index of π-delocalization $\langle\lambda\rangle$ is calculated as $\langle\lambda\rangle = \Sigma_{i=1}^{N}\lambda_i/N$ where N is the number of conjugated bonds and λ_i is calculated as $\lambda_i = n_i - 1$ or $\lambda_i = 2 - n_i$ for formal single and double bonds, respectively.

*[4,4′]NON (**2.III**).* Similar behaviour is displayed by the double-enaminones [4,4′]NON (**2.III**). The analysis has been restricted to non-annulated enaminones with simple aliphatic or aromatic substituents (**2.IIa**), a class of molecules known to form rather weak RAHBs with N···O distances around 2.66 Å but with large π-delocalizations of the resonant fragment, both facts attributable to the heteronuclear nature of the N—H···O bond (see below) (Gilli *et al.*, 2000, 2002). Comparison between single (**2.IIa**) and double (**2.III**) enaminones shows that the effect of π-bond anticooperativity, though apparently unable to lengthen the already weak N—H···O bond of some 2.66 Å, can still be detected from the large decrease of π-delocalization of the resonant fragment which is 76% in **2.IIa** and only 55% (on average) in **2.III** (Table 1).

*[4,4′]NOO (**2.II**).* Both [4,4′]OOO and [4,4′]NON patterns **2.I** and **2.III** form symmetrical O—H···O···H—O or N—H···O···H—N schemes where the two bonds compete equally for the central atom according to the simple rules given above. This symmetry is lost in [4,4′]NOO (**2.II**) where the two hydrogen bonds in the N—H···O···H—O arrangement are different. The effect of this imbalance can be appreciated by comparing the geometry of the fused pattern **2.II** with those of the N—H···O (**2.IIa**) and O—H···O (**2.IIb**) building blocks, forming the HB1 and HB2 bonds, respectively (Scheme 2*A* and Table 1). $d_{\rm N\cdots O}$(HB1) is substantially unchanged by the ring fusion (from 2.66 to 2.65 Å) while $d_{\rm O\cdots O}$(HB2) is shortened from 2.47 to 2.42 Å, apparently against any ring anticooperativity effect. At the same time, the π-delocalization of the β-enaminone increases from 76 to 88%, while that of the enolone decreases from 70 to 58%.

Interpretation of these results needs to make reference to the basic reasons why RAHB can strengthen the hydrogen bond (Gilli *et al.*, 2004, 2005). Really strong $D\cdots{\rm H}\cdots A$ bonds (*i.e.* true three-centre–four-electron covalent bonds) can only occur when the proton has strictly comparable affinity for the donor D and the acceptor A, *i.e.* when $\Delta{\rm p}K_{\rm a} = {\rm p}K_{\rm a}(D{-}H) - {\rm p}K_{\rm a}(A{-}{\rm H}^+) \simeq 0$.[5] In general, hydrogen bonds such as R—OH···O═C are weak because of the huge p$K_{\rm a}$ difference between alcohols and ketones, which amounts to 20–25 p$K_{\rm a}$ units (Maskill, 1985; Smith & March, 2001). This difference, however, can be reduced by delocalization of the interleaving resonant fragment, and eventually annihilated when such a delocalization becomes complete (Del% = 100). $\Delta{\rm p}K_{\rm a}$ is even greater for the R—N(R)—H···O═C bond, being, with respect to ketones, 43–48 and 31–38 p$K_{\rm a}$ units for amines and anilines, respectively. As a consequence, the N—H···O RAHB in **2.IIa** is much longer (2.66 Å) than the corresponding O—H···O bond in **2.IIb** (2.47 Å) although slightly more delocalized (76% against 70%). Accordingly, $\Delta{\rm p}K_{{\rm a},R}$, the residual $\Delta{\rm p}K_{\rm a}$ left after RAHB formation, must remain significantly larger for the N—H···O bond than for O—H···O bond. When the two RAHB rings are connected in **2.II**, this $\Delta{\rm p}K_{{\rm a},R}$ difference becomes the driving chemical potential, $\Delta\mu$, that determines what will happen. Accordingly, the anticooperative fusion **2.IIa** + **2.IIb** ⇒ **2.II** induces a further delocalization of the enaminone fragment (from 76% to 88%) which is not used to strengthen the N—H···O bond but rather to set up a larger negative charge on the carbonyl oxygen which decreases $\Delta\mu$ by decreasing the difference of $\Delta{\rm p}K_{\rm a}$ between N—H and C═O. In the mean time, the negative charge set on the central oxygen reduces $\Delta{\rm p}K_{\rm a}$ between the O—H and C═O groups of the adjacent enolone causing a shortening of the O—H···O bond from 2.47 to 2.42 Å without any need of further enolone delocalization (which is actually decreased from 70 to 58%).

3.2. Enolone–enolone fusion through the C—C bond

The fusion of two enolone rings through a C—C bond gives rise (Fig. 1) to the π-anticooperative pattern [2,2′]OOOO and to a couple of π-cooperative patterns, [3,2′]OOOO ⇌ [2,3′]OOOO, which are symmetry related and then isoenergetic whenever symmetrically substituted. The system was first studied by Destro & Marsh (1984) in citrinin (**3.IVa**), a natural product of vegetal origin, showing that the configuration adopted was the cooperative one and that the two hydrogen-bonded protons were ordered below 147 K but disordered over four positions above 147 K. Later it was shown (Destro, 1991) by combined use of van't Hoff plots and variable-temperature X-ray crystallography that the energy difference between the two disordered positions was only 6.70 kJ mol^{-1}. The general schemes **2.IVa** and **2.IVb** ([3,2′]OOOO or [2,3′]OOOO configuration, disorder at room temperature and ordering at lower temperatures) were confirmed by the small number of structures determined later (Sugawara *et al.*, 1992; Mochida *et al.*, 1992; Roversi *et al.*, 1996; Shishkina *et al.*, 2002; Duncan *et al.*, 2002) for citrinin-like compounds. The mean geometrical parameters for both ordered and disordered structures are summarized in Table 1.

The occurrence of the π-bond cooperative pattern [3,2′]OOOO instead of the anticooperative pattern is fully confirmed by the lengths of the shared C—C bond [1.47 (1) Å in both ordered and disordered structures] typical of a pure C(sp^2)—C(sp^2) single bond (Allen *et al.*, 1987). The RAHB cycle now runs all around the two fused rings with a global π-delocalization, measured in the ordered form, of 64%. The double hydrogen bond formed is then a RAHB of a new type that can be indicated as (R_1 + R_3)-RAHB because the two resonant fragments R_n now have different lengths (1 and 3, respectively). Both O—H···O bonds are remarkably strong [$d_{\rm O\cdots O}$(HB1) = 2.54 and $d_{\rm O\cdots O}$(HB2) = 2.48 Å], suggesting that this cooperative pattern is endowed with a particular stability. The much higher delocalization of the disordered form **2.IVb** (94%) is actually an artifact (Gilli *et al.*, 2004) produced by a combination of static or dynamic disorder and insufficient resolution of present diffraction experiments that, while able to distinguish the rather distant positions of the disordered proton, cannot resolve the close but equally

---

[5] An identical criterion makes use of the concept of proton affinity, PA, so that the equation becomes $\Delta{\rm PA} = {\rm PA}(D^-) - {\rm PA}(A) \simeq 0$. The two relationships are logically equivalent but ΔPA is more properly defined in the gas phase, while $\Delta{\rm p}K_{\rm a}$ is believed to be more appropriate in water solutions and other condensed phases such as crystals.

disordered positions of the heavy atoms belonging to the two overlapping resonant fragments of the tautomeric equilibrium **2.IVb**.

3.3. Enolone–enaminone and enaminone–enaminone fusion through the C—C bond

In theory, the resonant enaminone fragment is compatible with both N—H···O and O—H···N bonds. In practice, the latter is never observed in these compounds because of the much higher affinity of the proton for the nitrogen with respect to oxygen (Gilli *et al.*, 2000). On the other hand, it is well established (Olivieri *et al.*, 1989; Gilli *et al.*, 2000, 2002, 2005, 2006) that intramolecular O—H···N RAHBs can be stabilized only by fusion of the hydrogen-bonded ring with an aromatic one [as, for instance, in 1-(arylazo)-2-phenols or -2-naphthols], which is sterically impossible in the fused double-rings considered here. C—C bond fusion of enolone and enaminone groups can therefore occur only (Fig. 1) according to the tautomeric patterns [2,2′]OONO and [3,2′]OONO, which are π-anticooperative and cooperative, respectively, together with the non-tautomeric cooperative isomer [2,3′]OONO. The molecules of interest are sketched in **2.Va**–**2.Vc** of Scheme 2*B* and the corresponding mean geometrical parameters are given in Table 1.

At variance with the citrinin-like compounds discussed above, both anticooperative and cooperative tautomers [2,2′]OONO $\rightleftharpoons$ [3,2′]OONO (**2.Va** $\rightleftharpoons$ **2.Vb**) are observed, though in the uneven ratio of five to 18 cases, while the cooperative stereoisomer [2,3′]OONO (**2.Vc**) is found only once (Table 1). The different occurrences of the two tautomers suggest that the latter is more stable than the former, consistent with the fact that the anticooperative [2,2′]OONO pattern is endowed with longer hydrogen-bond distances and smaller π-delocalizations ($d_{\mathrm{O}\cdots\mathrm{O}}$ = 2.48 Å, $d_{\mathrm{N}\cdots\mathrm{O}}$ = 2.70 Å and Del% = 70) than the corresponding [3,2′]OONO cooperative pattern ($d_{\mathrm{O}\cdots\mathrm{O}}$ = 2.44 Å, $d_{\mathrm{N}\cdots\mathrm{O}}$ = 2.66 Å and Del% = 78).[6] In agreement with citrinines, the π-cooperative nature of both [3,2′]OONO (**2.Vb**) and [2,3′]OONO (**2.Vc**) patterns can be seen from the bond distance of the C—C bond connecting the two delocalized systems, which is 1.46 Å (n = 1.14) and 1.47 Å (n = 1.09), respectively, and corresponds to a pure C(sp^2)—C(sp^2) single bond (Allen *et al.*, 1987).

The fusion of two enaminones through a C—C bond can be achieved in two different ways, NN-*trans* and NN-*cis* with respect to the C—C connection. Because of the instability of O—H···N bonds, the *trans* form can only give rise to the cooperative [3,2′]NONO pattern (Fig. 1) and, in fact, all of the few compounds retrieved (Takahashi *et al.*, 1989; Mehdi, 1990) adopt this cooperative scheme (**2.VI**), which is essentially the *trans* fusion of two simple enaminones **2.IIa** with similar π-delocalizations and some shortening of one of the two hydrogen bonds (2.59 instead of 2.66 Å).

The behaviour of the NN-*cis* isomer, of which only three examples have been retrieved (Adhikesavalu & Venkatesan, 1983; Bernhardt *et al.*, 2002), is completely different. They do not adopt the expected neutral pattern [2,2′]NONO (Fig. 1) but the double zwitterionic form [2,2′]$\mathrm{NN^{+}OO^{-}}$ (see **2.VII** in Scheme 2*B*). Two ions are formed, the $[\mathrm{H{-}N}\overset{\cdots}{-}\mathrm{C}\overset{\cdots}{-}\mathrm{N{-}H}]^{+}$ amidinium cation and the $[\mathrm{O}\overset{\cdots}{-}\mathrm{C}\overset{\cdots}{-}\mathrm{C}\overset{\cdots}{-}\mathrm{C}\overset{\cdots}{-}\mathrm{O}]^{-}$ β-diketonate anion, which are internally almost completely π-delocalized (Del% of 92 and 100, respectively) and, facing each other, form two charged $\mathrm{N^{1/2+}{-}H\cdots O^{1/2-}}$ bonds of 2.66 Å. The prevalence of the zwitterionic form can be attributed to the stability of the amidinium cation and β-diketonate anion (Bertolasi *et al.*, 2002), both ions strongly stabilized by resonance, together with the relative instability of the neutral form [2,2′]NONO because of its anticooperative nature.

4. Experimental section

X-ray diffraction data were collected at room temperature for (1)–(4) and at 100 K for (5) according to the experimental details of Table 2. Data sets were integrated using the *Denzo-SMN* package (Otwinowski & Minor, 1997). Structures were solved by direct methods (*SIR*97: Altomare *et al.*, 1999) and refined (*SHELXL*97: Sheldrick, 1997) by full-matrix least-squares methods with anisoptropic non-H and isotropic H atoms, with the exception of (5) for which the $\mathrm{O_1\cdots H\cdots O_2}$ proton was also treated anisotropically. All remaining calculations were performed using the program *PARST* (Nardelli, 1995). *ORTEP* (Burnett & Johnson, 1996) views with ellipsoids at 40% probability are shown in Fig. 3. Selected bond distances and hydrogen-bond parameters are given in Tables 3 and 4. Complete crystallographic data are available from the deposited CIF files.

5. Discussion and perspectives

RAHB has been known since 1989 as a synergistic reinforcement of hydrogen-bond strength and delocalization of the π-conjugated chain connecting hydrogen-bond donor and acceptor atoms (Gilli *et al.*, 1989, 2004; Bertolasi *et al.*, 1996). In general, the idea of RAHB has been well accepted by the scientific community and has been used in the most recent hydrogen-bond books (Jeffrey, 1997; Desiraju & Steiner, 1999) and reviews (Steiner, 2002; Sobczyk *et al.*, 2005). Moreover, a recent survey by Allen, Howard and co-workers has verified that the most frequent intramolecular ring motifs observed in crystals are actually ‘planar, six-membered conjugated systems stabilized by RAHB’ (Bilton *et al.*, 2000). Over the years, the RAHB effect has been interpreted differently in terms of movements of partial charges (Gilli *et al.*, 1989), resonance between keto–enol and enol–keto VB canonical forms (Gilli *et al.*, 1994), electron effective masses within the hydrogen bond and in the conjugated segment (Munn & Eckhardt, 2001), Marcus rate-equilibrium theory (Gilli *et al.*, 2002, 2005, 2006), Bader AIM analysis (Bader, 1990; Bader & Gatti, 1998) of electron densities (Madsen *et al.*, 1998; Schiøtt *et al.*, 1998; Gilli *et al.*, 2002; Gatti *et al.*, 2003) and state-correlation (or

---

[6] The reason why molecules choose the less stable anticooperative pattern in five of the 23 cases seems to depend on their chemical specificities, four being tetracyclines protonated at the 4-$\mathrm{NMe_2}$ group (Scheme **1.V** and **3.Va**) and the other being a 1,3-dioxane-4,6-dione which embeds two esteric, instead of carbonylic, functions (Scheme **3.Va′**).

avoided-crossing) diagrams (Gilli *et al.*, 2004), not to mention the second-order Jahn–Teller effect treatment made by Haddon in 1980, that was nine years before the acronym RAHB was proposed (Haddon, 1980).

Probably the most general explanation remains the PA/pK_a equalization principle, a simple idea that arose in the early 1970s (Pimentel, 1951; Malarski *et al.*, 1982; Meot-Ner (Mautner), 1984, 1987; Zeegers-Huyskens, 1986; Huyskens *et al.*, 1991) and generally accepted now, by which the hydrogen-bond strength is essentially determined, besides the high electronegativity of the hydrogen-bond donor and acceptor atoms, by the difference between their proton affinities (ΔPA) or acid–base dissociation constants (ΔpK_a), the hydrogen bond being the stronger and more covalent the smaller this difference is. From this point of view, the RAHB strengthening arises from the fact that the increasing π-delocalization of the interleaving heterodiene reduces the PA/pK_a difference between the terminal heteroatoms and, at least in the X—H$\cdots X$ homonuclear bond, can make them identical (Gilli *et al.*, 2004, 2005, 2006).

The two concepts of ‘synergism of hydrogen-bond strengthening and π-delocalization’ and of ‘PA/pK_a equalization’ should therefore be sufficient to interpret any aspect of RAHB and, in fact, the present paper has shown that they can also be used to analyze combinations of two RAHB rings and to explain successfully the relative stabilities of all possible tautomers arising from them. The discussion has raised some interesting points:

(i) There has been some discussion (Steiner, 2002) on the possibility of π-bond anticooperative effects on the hydrogen-bond strength. The present analysis has shown that such effects are actually detectable for the O—H$\cdots$O$\cdots$H—O and N—H$\cdots$O$\cdots$H—N symmetrical arrangements which compete for the central C═O bond (patterns [4,4′]OOO and [4,4′]NON). A more complex anticooperative effect is observed for the N—H$\cdots$O$\cdots$H—O asymmetric arrangement associated with the [4,4′]NOO pattern, where the fusion weakly affects the N—H$\cdots$O bond while considerably strengthening the O—H$\cdots$O bond. This new effect has also proved to be likely to interpretation by making use of the PA/pK_a equalization concept.

(ii) The [*n,n*′]*XXXX* family of patterns gives rise to 15 potential tautomers. The presence of N—H$\cdots$O or O—H$\cdots$N bonds is the main determinant of their occurrence, only the former being actually observed in the current set of data. The most interesting point is that some of the observed tautomers differ in energy for a reason that, to our knowledge, has never been discussed before in the chemical literature. This happens for the two couples of [2,2′]OOOO/[3,2′]OOOO and [2,2′]OONO/[3,2′]OONO patterns which are observed in the ratios 0/8 and 5/18, respectively, and whose different occurrences and stabilities can only be attributed to the rather curious fact that the resonant bonds follow different π-conjugated pathways within the two forms of the couple. The higher-energy form corresponds to the π-anticooperative (R_3/R_3)-RAHB built up by two R_3-RAHB rings joined in antidromic fashion. The lower-energy form is π-cooperative and consists of the unique homodromic ten-membered RAHB ring that we have indicated above as (R_1 + R_3)-RAHB. The results suggest the idea of a novel type of cooperative–anticooperative prototropic tautomerism.

(iii) Finally, some applications of these compounds in the field of functional materials can be envisaged. All [*n,n*′]*XXXX* RAHB patterns are potential multi-state systems switchable from one state to another by coordinated proton transfer (PT) and interchange of the single and double bonds within the resonant spacer. Since the N—H$\cdots$O $\rightleftharpoons$ O—H$\cdots$N tautomerism is inactive in this class of compounds, PT remains confined to the O—H$\cdots$O bonds, which are certainly short enough (Table 1) to be endowed with a double-well potential of low PT-barrier (LBHB = low-barrier hydrogen bond) (Cleland, 1992; Cleland & Kreevoy, 1994; Frey *et al.*, 1994; Frey, 2001; Harris & Mildvan, 1999). In particular, the two [2,2′]OOOO $\rightleftharpoons$ [3,2′]OOOO $\rightleftharpoons$ [2,3′]OOOO and [2,2′]OONO $\rightleftharpoons$ [3,2′]OONO tautomeric equilibria are associated with molecular fragments having permanent dipole moments differently oriented in the different tautomers and possibly likely to be voltage-operated. Scheme 5 shows the dipole moments μ (in D) of these tautomers as evaluated by the semi-empirical Gasteiger method.[7]

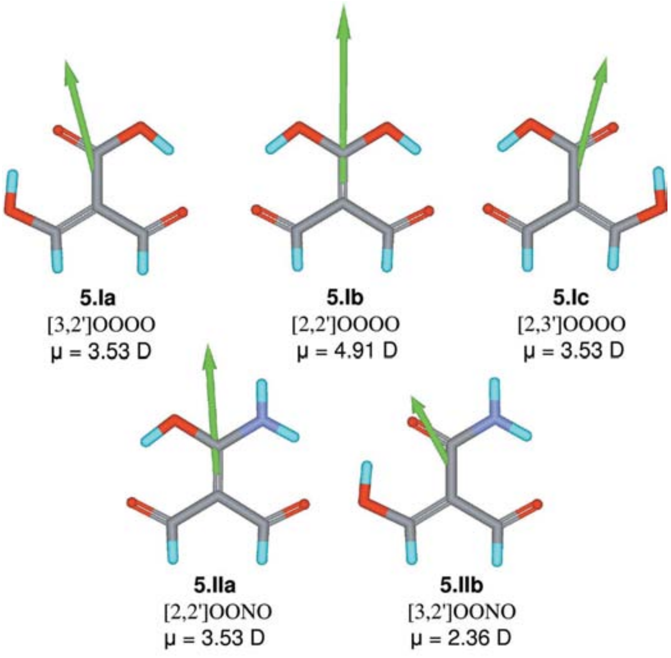

Scheme 5

Of greater interest is the [3,2′]OOOO $\rightleftharpoons$ [2,3′]OOOO equilibrium which is endowed with a horizontal invertible component of the dipole moment of some 0.9 D. Crystal structures have shown that these crystals have disordered protons at room temperature, becoming ordered at lower temperatures (Destro & Marsh, 1984; Destro, 1991),

---

[7] Dipole moments have been evaluated by means of the *DS ViewerPro* 5.0 (Accelrys, 2002) set of programs using geometries optimized by molecular mechanics and partial atomic charges calculated according to Gasteiger & Marsili (1980).

Table 2
Experimental details.

	(1)	(2)	(3)	(4)	(5)
Crystal data					
Chemical formula	$C_{15}H_{12}O_3$	$C_{15}H_{11}ClO_3$	$C_{16}H_{14}O_3$	$C_{16}H_{13}ClO_3$	$C_{14}H_{13}HClNO_6$
M_r	240.25	274.69	254.27	288.71	327.71
Cell setting, space group	Monoclinic, *C*2/*c*	Monoclinic, $P2_1/n$	Orthorhombic, $Pca2_1$	Monoclinic, $P2_1/n$	Triclinic, $P\bar{1}$
Temperature (K)	295	295	295	295	100
a, *b*, *c* (Å)	27.299 (2), 5.4343 (2), 17.576 (1)	13.932 (1), 5.3108 (2), 17.878 (1)	17.602 (1), 6.8423 (2), 21.662 (1)	14.147 (1), 5.3300 (3), 18.618 (2)	5.6849 (1), 9.0280 (2), 14.8742 (4)
α, β, γ (°)	90.00, 116.215 (2), 90.00	90.00, 105.137 (3), 90.00	90.00, 90.00, 90.00	90.00, 104.777 (4), 90.00	74.923 (1), 83.543 (2), 71.815 (2)
V (Å^3)	2339.2 (3)	1276.9 (1)	2609.0 (2)	1357.4 (2)	699.89 (3)
Z	8	4	8	4	2
D_x (Mg m^{-3})	1.364	1.429	1.295	1.413	1.555
Radiation type	Mo $K\alpha$	Mo $K\alpha$	Mo $K\alpha$	Mo $K\alpha$	Mo $K\alpha$
No. of reflections for cell parameters	4754	5187	16 585	5414	6530
μ (mm^{-1})	0.10	0.30	0.09	0.28	0.30
Crystal form, colour	Prism, yellow	Prism, yellow	Prism, yellow	Prism, yellow	Prismatic, colourless
Crystal size (mm)	0.26 × 0.12 × 0.10	0.33 × 0.12 × 0.09	0.26 × 0.21 × 0.14	0.48 × 0.11 × 0.07	0.52 × 0.35 × 0.16
Data collection					
Diffractometer	Nonius Kappa CCD	Nonius Kappa CCD	Nonius Kappa CCD	Nonius Kappa CCD	Nonius Kappa CCD
Data collection method	φ scans and ω scans	φ scans and ω scans	φ scans and ω scans	φ scans and ω scans	φ scans and ω scans
Absorption correction	None	None	None	None	None
$T_{\min}$	–	–	–	–	–
$T_{\max}$	–	–	–	–	–
No. of measured, independent and observed reflections	4754, 2663, 1862	5187, 2903, 2098	16 585, 5825, 3242	5414, 3078, 2210	14 589, 4119, 3680
Criterion for observed reflections	$I > 2\sigma(I)$	$I > 2\sigma(I)$	$I > 2\sigma(I)$	$I > 2\sigma(I)$	$I > 2\sigma(I)$
$R_{\rm int}$	0.031	0.036	0.066	0.049	0.031
$\theta_{\max}$ (°)	27.5	27.5	28.0	27.5	30.5
Refinement					
Refinement on	F^2	F^2	F^2	F^2	F^2
$R[F^2 > 2\sigma(F^2)]$, $wR(F^2)$, S	0.055, 0.147, 1.11	0.055, 0.155, 1.11	0.052, 0.128, 1.00	0.055, 0.160, 1.12	0.035, 0.084, 1.10
No. of parameters	211	216	455	233	260
H-atom treatment	Refined independently	Refined independently	Refined independently	Refined independently	Refined independently
Weighting scheme	$w = 1/[\sigma^2(F_o^2) + (0.0596P)^2 + 0.7909P]$, where $P = (F_o^2 + 2F_c^2)/3$	$w = 1/[\sigma^2(F_o^2) + (0.0628P)^2 + 0.4171P]$, where $P = (F_o^2 + 2F_c^2)/3$	$w = 1/[\sigma^2(F_o^2) + (0.0564P)^2]$, where $P = (F_o^2 + 2F_c^2)/3$	$w = 1/[\sigma^2(F_o^2) + (0.0652P)^2 + 0.3211P]$, where $P = (F_o^2 + 2F_c^2)/3$	$w = 1/[\sigma^2(F_o^2) + (0.0241P)^2 + 0.393P]$, where $P = (F_o^2 + 2F_c^2)/3$
$(\Delta/\sigma)_{\max}$	0.001	<0.0001	0.002	<0.0001	0.001
$\Delta\rho_{\max}$, $\Delta\rho_{\min}$ (e Å^{-3})	0.16, −0.18	0.19, −0.31	0.16, −0.15	0.19, −0.42	0.36, −0.36
Extinction method	None	None	*SHELXL*	None	None
Extinction coefficient	–	–	0.0147 (14)	–	–
Absolute structure	–	–	Flack (1983)	–	–
Flack parameter	–	–	0.7 (11)	–	–

Computer programs used: *Kappa-CCD server software* (Nonius, 1997), *Denzo-SMN* (Otwinowski & Minor, 1997), *SIR*97 (Altomare *et al.*, 1999), *SHELXL*97 (Sheldrick, 1997), *ORTEP*III (Burnett & Johnson, 1996), *PARST* (Nardelli, 1995).

Table 3
Selected bond distances (Å).

	C1—O1	C1—C2	C2—C3	C3—O2	C1—C10	C10—C11	C11—O3
(1)	1.268 (2)	1.431 (2)	1.362 (3)	1.322 (2)	1.474 (2)	1.409 (2)	1.348 (2)
(2)	1.262 (3)	1.428 (3)	1.359 (3)	1.320 (3)	1.478 (3)	1.405 (3)	1.346 (3)
(3)	1.275 (4)	1.430 (5)	1.357 (4)	1.335 (4)	1.469 (4)	1.404 (4)	1.362 (4)
	1.260 (4)	1.433 (5)	1.358 (4)	1.322 (4)	1.472 (4)	1.414 (4)	1.349 (4)
(4)	1.267 (4)	1.432 (4)	1.354 (3)	1.327 (3)	1.469 (3)	1.416 (3)	1.348 (4)

	C1—O1	C1—C2	C2—C3	C3—O2	C1—N1	C2—C4	C4—O3	C6···O6
(5)	1.263 (1)	1.477 (2)	1.398 (2)	1.306 (1)	1.344 (2)	1.472 (1)	1.223 (2)	2.598 (1)

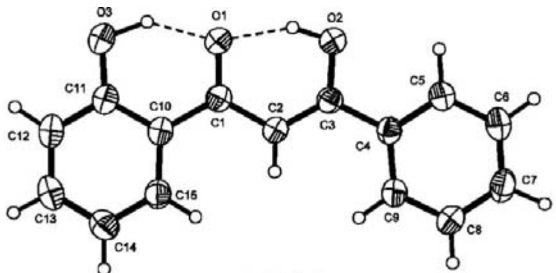

1 (295 K)

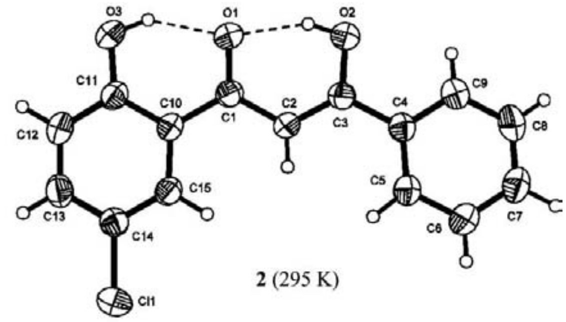

2 (295 K)

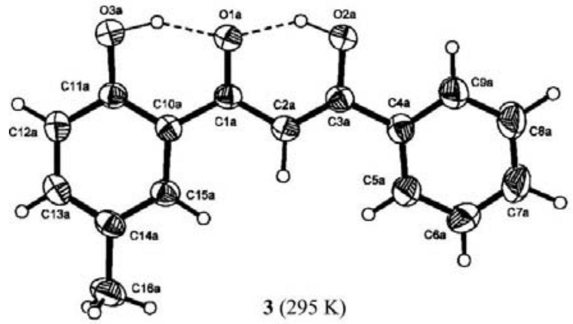

3 (295 K)

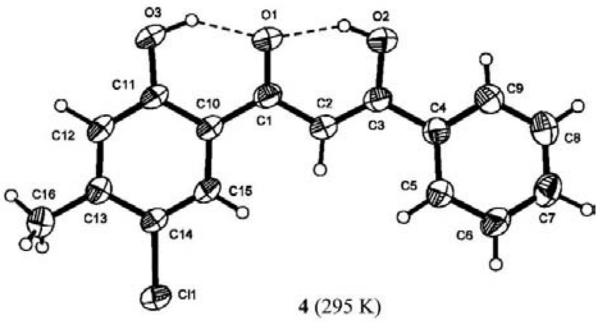

4 (295 K)

Table 4
Hydrogen-bonding parameters (Å, °).

	D—H	H···A	D···A	D—H···A	δ_{OH} (p.p.m.)†
(1)					
O2—H···O1	0.94 (2)	1.66 (3)	2.530 (2)	151 (3)	15.6
O3—H···O1	1.07 (3)	1.64 (3)	2.575 (2)	143 (3)	12.1
O2—H···O1^{i}	0.94 (2)	2.45 (2)	2.885 (2)	108 (2)	
O3—H···O2^{i}	1.07 (3)	2.42 (4)	3.180 (2)	127 (2)	
(2)					
O2—H···O1	0.86 (4)	1.75 (3)	2.543 (3)	152 (3)	15.5
O3—H···O1	0.88 (4)	1.81 (4)	2.586 (2)	146 (4)	12.1
O2—H···O1^{ii}	0.86 (4)	2.44 (4)	2.844 (3)	110 (3)	
O3—H···O2^{ii}	0.88 (4)	2.47 (4)	3.133 (3)	132 (2)	
(3)					
O2A—H···O1A	1.00 (4)	1.62 (4)	2.509 (3)	145 (4)	15.6
O2B—H···O1B	0.98 (4)	1.61 (4)	2.512 (3)	151 (4)	
O3A—H···O1A	1.06 (4)	1.57 (4)	2.569 (3)	154 (4)	11.9
O3B—H···O1B	0.95 (4)	1.73 (4)	2.571 (3)	146 (4)	
O2A—H···O1B	1.00 (4)	2.32 (4)	2.847 (4)	112 (3)	
O2B—H···O1A	0.98 (4)	2.40 (4)	2.866 (3)	108 (3)	
O3A—H···O2B	1.06 (4)	2.46 (4)	3.110 (3)	119 (3)	
O3B—H···O2A	0.95 (4)	2.42 (4)	3.090 (3)	128 (3)	
(4)					
O2—H···O1	0.90 (5)	1.73 (4)	2.552 (3)	148 (4)	15.5
O3—H···O1	0.98 (4)	1.73 (4)	2.588 (3)	144 (4)	12.0
O2—H···O1^{iii}	0.90 (4)	2.43 (5)	2.926 (3)	114 (3)	
O3—H···O2^{ii}	0.98 (4)	2.44 (4)	3.143 (3)	128 (3)	
(5)					
O2—H···O1	1.01 (3)	1.46 (3)	2.418 (1)	157 (2)	16.8
N1—H···O3	0.89 (2)	1.85 (2)	2.621 (1)	143 (2)	10.5

Symmetry codes: (i) $2 - x, -y - 1, -z$; (ii) $-x, -y - 1, -z$; (iii) $2 - x, -y, -z$.
† ^{1}H NMR pattern collected in $CDCl_3$ solution on a Varian Gemini 300.

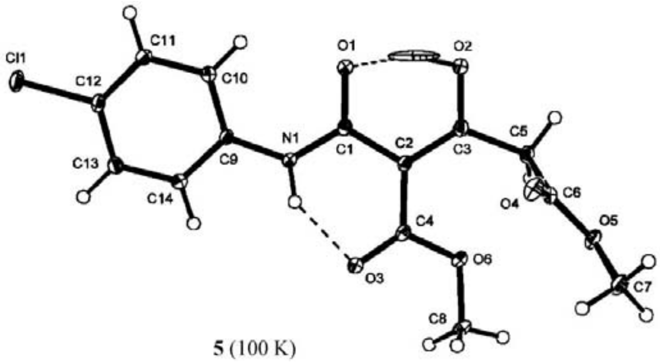

5 (100 K)

Figure 3
*ORTEP*III (Burnett & Johnson, 1996) views of the crystal structures determined at room temperature (1)–(4) and and at 100 K (5). Displacement ellipsoids are drawn at 40% probability.

suggesting that they may display a disorder–order phase transition at low temperature of possible paraelectric to ferro-/antiferroelectric nature. So far only two such molecules have been tested, 2-carboxy-3-hydroxy-phenalen-1-one (**3.IVb**) (Sugawara *et al.*, 1992) and 7-hydroxy-5-oxo-5H-dibenzo-[*a*,*c*][7]annulene-6-carboxylic acid (**3.IVb′**) (Mochida *et al.*, 1992), of which only the first displays antiferroelectric ordering below 40 K, while the second does not, most probably because the O—H···O bond is so short (O···O = 2.40 Å) to achieve single-well PT profile (Gilli *et al.*, 2004) and to lose, therefore, two-state properties.

We thank MIUR (Rome) for COFIN 2004 financial support in the frame of our project 'Smart Hydrogen Bonds in Nature and in Functional Materials', and Professor Augusto Cesare Veronese, Dipartimento di Scienze Farmaceutiche, Università di Ferrara, for providing crystals of (5).

References

Accelrys (2002). *DS ViewerPro.* Version 5.0. Accelrys Inc., San Diego, California, USA.

Adhikesavalu, D. & Venkatesan, K. (1983). *Acta Cryst.* C**39**, 1044–1048.

Agre, P., Lee, M. D., Devidas, S. & Guggino, W. B. (1997). *Science*, **275**, 1490–1492.

Allen, F. H. (2002). *Acta Cryst.* B**58**, 380–388.

Allen, F. H., Kennard, O., Watson, D. G., Brammer, L., Orpen, A. G. & Taylor, R. (1987). *J. Chem. Soc. Perkin Trans. 2*, pp. S1–S19.

Altomare, A., Burla, M. C., Camalli, M., Cascarano, G. L., Giacovazzo, C., Guagliardi, A., Moliterni, A. G., Polidori, G. & Spagna, R. (1999). *J. Appl. Cryst.* **32**, 115–119.

Bader, R. F. W. (1990). *Atoms in Molecules – A Quantum Theory.* Oxford University Press.

Bader, R. F. W. & Gatti, C. (1998). *Chem. Phys. Lett.* **287**, 233–238.

Bartoli, G., Bosco, M., Cimarelli, C., Dalpozzo, R., De Munno, G., Guercio, G. & Palmieri, G. (1992). *J. Org. Chem.* **57**, 6020–6025.

Bernhardt, P. V., Koch, R., Moloney, D. W. J., Shtaiwi, M. & Wentrup, C. (2002). *J. Chem. Soc. Perkin Trans. 2*, pp. 515–523.

Bertolasi, V. & Ferretti, V. (2005). *Encyclopedia of Supramolecular Chemistry*, edited by J. L. Atwood & J. Steed, pp. 1–19. New York: Marcel Dekker.

Bertolasi, V., Gilli, P., Ferretti, V. & Gilli, G. (1991). *J. Am. Chem. Soc.* **113**, 4917–4925.

Bertolasi, V., Gilli, P., Ferretti, V. & Gilli, G. (1995). *Acta Cryst.* B**51**, 1004–1015.

Bertolasi, V., Gilli, P., Ferretti, V. & Gilli, G. (1996). *Chem. Eur. J.* **2**, 925–934.

Bertolasi, V., Gilli, P., Ferretti, V. & Gilli, G. (1997). *J. Chem. Soc. Perkin Trans. 2*, pp. 945–952.

Bertolasi, V., Pretto, L., Gilli, P., Ferretti, V. & Gilli, G. (2002). *New J. Chem.* **26**, 1559–1566.

Bilton, C., Allen, F. H., Shields, G. P. & Howard, J. A. K. (2000). *Acta Cryst.* B**56**, 849–856.

Bordner, J. (1979). *Acta Cryst.* B**35**, 219–222.

Bossio, R., Marcaccini, S., Paoli, P., Pellegrini, G., Pepino, R. & Torroba, T. (1993). *J. Chem. Res. (S)*, pp. 66–67.

Brbot-Šaranović, A., Pavlović, G. & Cindrić, M. (2000). *Struct. Chem.* **11**, 65–76.

Brbot-Šaranović, A., Pavlović, G., Vrdoljak, V. & Cindrić, M. (2001). *Croat. Chem. Acta*, **74**, 441–454.

Brodersen, D. E., Clemons, W. M. Jr, Carter, A. P., Morgan-Warren, R. J., Wimberly, B. T. & Ramakrishnan, V. (2000). *Cell*, **103**, 1143–1154.

Burnett, M. N. & Johnson, C. K. (1996). *ORTEP*III, Report ORNL-6895. Oak Ridge National Laboratory, Tennessee, USA.

Carrondo, M. A. A. F. de C. T., Matias, P. M., Heggie, W. & Page, P. R. (1994). *Struct. Chem.* **5**, 73–77.

Cindrić, M., Vrdoljak, V., Kajfez, T., Novak, P., Brbot-Šaranović, A., Strukan, N. & Kamenar, B. (2002). *Inorg. Chim Acta*, **328**, 23–32.

Clegg, W. & Teat, S. J. (2000). *Acta Cryst.* C**56**, 1343–1345.

Cleland, W. W. (1992). *Biochemistry*, **31**, 317–319.

Cleland, W. W. & Kreevoy, M. M. (1994). *Science*, **264**, 1887–1890.

Cox, P. J., MacManus, S. M., Sharp, S. K., Adam, D. & Muir, K. W. (1993). *J. Crystallogr. Spectrosc. Res.* **23**, 431–435.

Cunningham, B. D. M, Lowe, P. R. & Threadgill, M. D. (1989). *J. Chem. Soc. Perkin Trans. 2*, pp. 1275–1283.

Desiraju, G. R. & Steiner, Th. (1999). *The Weak Hydrogen Bond in Structural Chemistry and Biology.* Oxford University Press.

Destro, R. (1991). *Chem. Phys. Lett.* **181**, 232–236.

Destro, R. & Marsh, R. E. (1984). *J. Am. Chem. Soc.* **106**, 7269–7271.

Duax, W. L., Pletnev, V. & Burkhart, B. M. (2003). *J. Mol. Struct.* **647**, 97–111.

Duncan, L. L., Patrick, B. O. & Brock, C. P. (2002). *Acta Cryst.* B**58**, 502–511.

Flack, H. D. (1983). *Acta Cryst.* A**39**, 876–881.

Frey, P. A. (2001). *Magn. Reson. Chem.* **39**, S190–S198.

Frey, P. A., Whitt, S. A. & Tobin, J. B. (1994). *Science*, **264**, 1927–1930.

Gasteiger, J. & Marsili, M. (1980). *Tetrahedron*, **36**, 3219–3228.

Gatti, C., Cargnoni, F. & Bertini, L. (2003). *J. Comput. Chem.* **24**, 422–436.

Gilli, G., Bellucci, F., Ferretti, V. & Bertolasi, V. (1989). *J. Am. Chem. Soc.* **111**, 1023–1028.

Gilli, G. & Bertolasi, V. (1990). *The Chemistry of Enols*, edited by Z. Rappoport, ch. 13, pp. 713–764. New York: John Wiley.

Gilli, G., Bertolasi, V., Ferretti, V. & Gilli, P. (1993). *Acta Cryst.* B**49**, 564–576.

Gilli, P., Bertolasi, V., Ferretti, V. & Gilli, G. (1994). *J. Am. Chem. Soc.* **116**, 909–915.

Gilli, P., Bertolasi, V., Ferretti, V. & Gilli, G. (2000). *J. Am. Chem. Soc.* **122**, 10405–10417.

Gilli, P., Bertolasi, V., Pretto, L., Antonov, L. & Gilli, G. (2005). *J. Am. Chem. Soc.* **127**, 4943–4953.

Gilli, P., Bertolasi, V., Pretto, L., Ferretti, V. & Gilli, G. (2004). *J. Am. Chem. Soc.* **126**, 3845–3855.

Gilli, P., Bertolasi, V., Pretto, L. & Gilli, G. (2006). *J. Mol. Struct.* **790**, 40–49.

Gilli, P., Bertolasi, V., Pretto, L., Lycka, A. & Gilli, G. (2002). *J. Am. Chem. Soc.* **124**, 13554–13567.

Gilli, P., Ferretti, V., Bertolasi, V. & Gilli, G. (1996). *Advances in Molecular Structure Research*, edited by I. Hargittai. & M. Hargittai, Vol. 2, pp. 67–102. Greenwich, CT: JAI Press.

Gilli, P., Ferretti, V. & Gilli, G. (1996). *Fundamental Principles of Molecular Modeling*, edited by W. Gans, A. Amann & J. C. A. Boeyens, pp. 119–141. New York: Plenum Press.

Gilli, G. & Gilli, P. (2000). *J. Mol. Struct.* **552**, 1–15.

Grotthuss, C. J. T. de (1806). *Ann. Chim.* **58**, 54–74.

Haddon, R. C. (1980). *J. Am. Chem. Soc.* **102**, 1807–1811.

Harris, T. K. & Mildvan, A. S. (1999). *Proteins*, **35**, 275–282.

Himmelsbach, M., Lintvedt, R. L., Zehetmair, J. K., Nanny, M. & Heeg, M. J. (1987). *J. Am. Chem. Soc.* **109**, 8003–8011.

Huyskens, P. L., Luck, W. A. & Zeegers-Huyskens, T. (1991). Editors. *Intermolecular Forces.* Berlin: Springer Verlag.

Jeffrey, G. A. (1984). *Inclusion Compounds*, edited by J. L. Atwood, J. E. D. Davies & D. D. MacNicol, Vol. 1, pp. 135–190. London: Academic Press.

Jeffrey, G. A. (1995). *Crystallogr. Rev.* **3**, 213–259.

Jeffrey, G. A. (1997). *An Introduction to Hydrogen Bonding.* New York: Oxford University Press.

Jeffrey, G. A. & Saenger, W. (1991). *Hydrogen Bonding in Biological Structures.* Berlin: Springer Verlag.

Kar, T. & Scheiner, S. (2004). *J. Phys. Chem. A*, **108**, 9161–9168.

Kobko, N. & Dannenberg, J. J. (2003). *J. Phys. Chem. A*, **107**, 10389–10395.

Kobko, N., Paraskevas, L., del Rio, E. & Dannenberg, J. J. (2001). *J. Am. Chem. Soc.* **123**, 4348–4349.

Kollat, V. & Stezowski, J. J. (1982). *Acta Cryst.* B**38**, 2531–2533.

Koziol, A. E., Davis, J., Palenik, R. C. & Palenik, G. J. (1992). *J. Crystallogr. Spectrosc. Res.* **22**, 493–501.

Madsen, G. K. H., Iversen, B. B., Larsen, F. K., Kapon, M., Reisner, G. M. & Herbstein, F. H. (1998). *J. Am. Chem. Soc.* **120**, 10040–10045.

Malarski, Z., Rospenk, M., Sobczyk, V & Grech, E. (1982). *J. Phys. Chem.* **86**, 401–406.

Maskill, H. (1985). *The Physical Basis of Organic Chemistry*, ch. 5, pp. 156–215. Oxford University Press.

Mehdi, S. (1990). *Acta Cryst.* C**46**, 2446–2447.

Meot-Ner (Mautner), M. (1984). *J. Am. Chem. Soc.* **106**, 1257–1264.

Meot-Ner (Mautner), M. (1987). *Molecular Structure and Energetics*, edited by J. F. Liebman & A. Greenberg, Vol. IV, ch. 3, pp. 71–103. Weinheim: VCH.

Mochida, T., Shiganawa, H., Izuoka, A. & Sugawara, T. (1992). *Chem. Lett.* **21**, 1623–1626.

Mukhopadhyaya, J. K., Sklenak, S. & Rappoport, Z. (2000*a*). *J. Am. Chem. Soc.* **122**, 1325–1336.

Mukhopadhyaya, J. K., Sklenak, S. & Rappoport, Z. (2000*b*). *J. Org. Chem.* **65**, 6856–6867.

Munn, R. W. & Eckhardt, C. J. (2001). *J. Phys. Chem. A*, **105**, 6938–6842.

Nardelli, M. (1995). *J. Appl. Cryst.* **28**, 659–660.

Ng, S. W., Othman, A. H. & Malek, S. N. A. (1994). *J. Chem. Cryst.* **24**, 331–335.

Nonius (1997). *Kappa-CCD Server Software.* Nonius BV, Delft, The Netherlands.

Olivieri, A. C., Wilson, R. B., Paul, I. C. & Curtin, D. Y. (1989). *J. Am. Chem. Soc.* **111**, 5525–5532.

Otwinowski, Z. & Minor, W. (1997). *Methods Enzymol.* **276**, 307–326.

Ozturk, S., Fun, H.-K., Akkurt, M., Sonmez, M. & Chinnakali, K. (1998). *Acta Cryst.* C**54**, IUC9800023.

Palenik, G. J., Mathew, M. & Restivo, R. (1978). *J. Am. Chem. Soc.* **100**, 4458–4464.

Pauling, L. (1947). *J. Am. Chem. Soc.* **69**, 542–553.

Pauling, L. (1960). *The Nature of the Chemical Bond*, 3rd ed. Ithaca, NY: Cornell University Press.

Pimentel, G. C. (1951). *J. Chem. Phys.* **19**, 446–448.

Pomès, R. & Roux, B. (2002). *Biophys. J.* **82**, 2304–2316.

Prewo, R. & Stezowski, J. J. (1980). *J. Am. Chem. Soc.* **102**, 7015–7020.

Prewo, R., Stezowski, J. J. & Kirchlechner, R. (1980). *J. Am. Chem. Soc.* **102**, 7021–7026.

Ried, W., Nenninger, J. & Bats, J. W. (1985). *Chem. Ber.* **118**, 1371–1382.

Roversi, P., Barzaghi, M., Merati, F. & Destro, R. (1996). *Can. J. Chem.* **74**, 1145–1161.

Saenger, W. (1979). *Nature (London)*, **279**, 343–344.

Saenger, W., Betzel, Ch., Hingerty, B. & Brown, G. M. (1982). *Nature (London)*, **296**, 581–583.

Scheiner, S. (1997). *Hydrogen Bonding: A Theoretical Perspective.* Oxford University Press.

Schiøtt, B., Iversen, B. B., Madsen, G. H. K. & Bruice, T. C. (1998). *J. Am. Chem. Soc.* **120**, 12117–12124.

Sheldrick, G. M. (1997). *SHELXL*97. University of Göttingen, Germany.

Shishkina, S. V., Shishkin, O. V., Ukrainets, I. V., Dakkah, A. N. & Sidorenko, L. V. (2002). *Acta Cryst.* E**58**, o254–o256.

Shishkina, S. V., Shishkin, O. V., Ukrainets, I. V., Jaradat, N. A. & Gorokova, O. V. (2000). *Acta Cryst.* C**56**, e168–e169.

Shuxiang, S., Decheng, G., Ying, C., Zonghua, Z., Zhihua, M. & Zhou, H. (1990). *Chin. J. Appl. Chem.* **7**, 78.

Silverton, J. V., Kabuto, C. & Akiyama, T. (1982). *Acta Cryst.* B**38**, 3032–3037.

Smith, M. B. & March, J. (2001). *March's Advanced Organic Chemistry*, 5th ed., ch. 8, pp. 327–362. New York: Wiley Interscience.

Sobczyk, L., Grabowski, S. J. & Krygowski, T. M. (2005). *Chem. Rev.* **105**, 3513–3560.

Steiner, T. (2002). *Angew. Chem. Int. Ed.* **41**, 48–76.

Steiner, Th. & Saenger, W. (1992). *Acta Cryst.* B**48**, 819–827.

Stezowski, J. J. (1976). *J. Am. Chem. Soc.* **98**, 6012–6018.

Sugawara, T., Mochida, T., Miyazaki, A., Izuoka, A., Sato, N., Sugawara, Y., Deguchi, K., Moritomo, Y. & Tokura, Y. (1992). *Solid State Commun.* **83**, 665–668.

Tajkhorshid, E., Nollert, P., Jensen, M. Ø., Miercke, L. J. W., O'Connell, J., Stroud, R. M. & Schulten, K. (2002). *Science*, **296**, 525–530.

Takahashi, T., Hirokami, S.-I., Nagata, M., Yamazaki, T. & Date, T. (1989). *J. Chem. Soc. Perkin Trans. 1*, pp. 1231–1239.

Taylor, R. & Kennard, O. (1984). *Acc. Chem. Res.* **17**, 320–326.

Taylor, R., Kennard, O. & Versichel, W. (1983). *J. Am. Chem. Soc.* **105**, 5761–5766.

Thailambal, V. G. & Pattabhi, V. (1985). *Acta Cryst.* C**41**, 802–804.

Ukrainets, I. V., Taran, S. G., Likhanova, N. V., Amin, D. N. & Shishkin, O. V. (2000). *Khim. Get. Soedin*, p. 64.

Ukrainets, I. V., Taran, S. G., Likhanova, N. V., Rybakov, V. B., Gorokhova, O. V. & Amin, J. N. (2000). *Khim. Get. Soedin.* p. 55.

Vishweshwar, P., Babu, N. J., Nangia, A., Mason, S. A., Puschmann, H., Mondal, R. & Howard, J. A. K. (2004). *J. Phys. Chem. A*, **108**, 9406–9416.

Von Dreele, R. B. & Hughes, R. E. (1971). *J. Am. Chem. Soc.* **93**, 7290–7296.

Wiley, P. F., Mizsak, S. A., Baczynskyj, L., Argoudelis, A. D., Duchamp, D. J. & Watt, W. J. (1986). *Org. Chem.* **51**, 2493–2499.

Zeegers-Huyskens, T. (1986). *J. Mol. Struct.* **135**, 93–103.